


Article

Modification of Nanocrystalline Porous Cu_{2-x}Se Films during Argon Plasma Treatment

Sergey P. Zimin^{1,2}, Ildar I. Amirov², Sergey V. Vasilev², Ivan S. Fedorov¹, Leonid A. Mazaletskiy¹ and Nam-Hoon Kim^{3,*} 

¹ Microelectronics and General Physics Department, Yaroslavl State University, 150003 Yaroslavl, Russia; zimin@uniyar.ac.ru (S.P.Z.); i.fedorov@uniyar.ac.ru (I.S.F.); l.mazaletskiy@uniyar.ac.ru (L.A.M.)

² Yaroslavl Branch of the Institute of Physics and Technology of Russian Academy of Sciences, 150007 Yaroslavl, Russia; ildamirov05428@gmail.com (I.I.A.); s.vasilev@uniyar.ac.ru (S.V.V.)

³ Department of Electrical Engineering, Chosun University, Gwangju 61452, Korea

* Correspondence: nhkim@chosun.ac.kr; Tel./Fax: +82-62-230-7028

Abstract: Cu_{2-x}Se films were deposited on Corning glass substrates by radio frequency (RF) magnetron sputtering and annealed at 300 °C for 20 min under N₂ gas ambient. The films had a thickness of 850–870 nm and a chemical composition of Cu_{1.75}Se. The initial structure of the films was nanocrystalline with a complex architecture and pores. The investigated films were plasma treated with RF (13.56 MHz) high-density low-pressure inductively coupled argon plasma. The plasma treatment was conducted at average ion energies of 25 and 200 eV for durations of 30, 60, and 90 s. Notably, changes are evident in the surface morphology, and the chemical composition of the films changed from x = 0.25 to x = 0.10 to x = 0.00, respectively, after plasma treatment at average ion energies of 25 and 200 eV, respectively.

Keywords: Cu_{2-x}Se films; plasma treatment; crystal structure; surface morphology



Citation: Zimin, S.P.; Amirov, I.I.; Vasilev, S.V.; Fedorov, I.S.; Mazaletskiy, L.A.; Kim, N.-H. Modification of Nanocrystalline Porous Cu_{2-x}Se Films during Argon Plasma Treatment. *Appl. Sci.* **2021**, *11*, 612. <https://doi.org/10.3390/app11020612>

Received: 24 November 2020

Accepted: 8 January 2021

Published: 10 January 2021

Publisher's Note: MDPI stays neutral with regard to jurisdictional claims in published maps and institutional affiliations.



Copyright: © 2021 by the authors. Licensee MDPI, Basel, Switzerland. This article is an open access article distributed under the terms and conditions of the Creative Commons Attribution (CC BY) license (<https://creativecommons.org/licenses/by/4.0/>).

1. Introduction

Nanostructured binary copper selenides have wide applications in various fields, such as solar cells, field-effect transistors, gas-sensing devices, Li-ion batteries, and biological and medical appliances [1–3]. Copper selenides have various stoichiometric (Cu₂Se, CuSe, Cu₃Se₂, CuSe₂, Cu₅Se₄) and nonstoichiometric (Cu_{2-x}Se) phases. There is special interest in the nonstoichiometric phase, owing to its unique properties. Cu_{2-x}Se is an intrinsic p-type semiconductor with direct and indirect bandgap energies in the range of 2.1–2.3 eV and 1.2–1.4 eV, respectively [4]. Non-stoichiometry affects the crystalline structure and the electronic and cation exchange properties. Nonstoichiometric nanostructured copper selenide may exhibit various morphologies, such as nanocubes [5], nanotubes [6], nanowires [7], nanosheets [8], nanodiscs [9], nanocages [10], and nanocrystalline films with complex architectures [11]. The type of nanostructure is determined by the formation methods and applied technological conditions. A detailed analysis of all the methods for Cu_{2-x}Se nanostructure creation is presented in [1]. Additionally, the properties of Cu_{2-x}Se nanostructures can be changed by thermal annealing or doping with various chemical elements. The plasma treatment of metal chalcogenides in argon plasma results in new phenomena associated with effective surface modification [12–14]. However, currently, no information about the effect of plasma treatment on the parameters of copper selenides exists in the literature. This study aims to analyze the effects of treatment by argon plasma with low ion energy on the structural parameters of nanocrystalline Cu_{2-x}Se films with complex architectures. An additional important physical problem investigated here is the poorly studied process of the plasma sputtering of discontinuous layers with pores.

2. Experimental Details

A commercial CuSe₂ alloy target (TASCO, 99.99% purity, 2-inch diameter) was used for preparing Cu_{2-x}Se thin film on 2 × 2 cm² Corning glass substrates. The thin films were deposited by radio frequency (RF) magnetron sputtering (IDT Engineering Co.) at room temperature using the following set of process parameters after pre-sputtering for 5 min [15]. The Ar gas flux was 50 sccm; the base pressure was 1.0 × 10⁻⁶ Torr; the substrate-to-target distance was 5.0 cm; the frequency was 13.56 MHz; the RF sputtering power was 35 W; and the vacuum pressure was 7.5 × 10⁻³ Torr during sputtering. After the growth process, the films were annealed using rapid thermal annealing (GD-Tech Co., GRT-100) at a temperature of 300 °C for 20 min under 10 sccm N₂ gas ambient. The thickness of the films was 850–870 nm.

The films were treated with RF high-density low-pressure inductively coupled plasma (ICP) at an RF of 13.56 MHz using an RF ICP reactor [16]. The experiments were performed with the following parameters. The inductive RF power *P* was 800 W; the argon gas flow was 10 sccm; the operating argon gas pressure was 0.07 Pa; and the RF bias powers to the substrate holder *P*_{sb} was 0 and 300 W. The ion energy was controlled by the RF bias power *P*_{sb} applied on the substrate. At RF bias powers of 0 and 300 W, the average ion energies were 25 and 200 eV, respectively. The ion current density was 7.5 mA cm⁻². The plasma treatment was conducted for durations of 30, 60, and 90 s. The plasma treatment of the sample involved bombarding the surface with normal incident argon ions accompanied by the heating of the surface and ultraviolet illumination of the argon plasma. The sample temperature during plasma treatment can increase by 100 °C at *P*_{sb} = 0 W and a processing duration of 60 s [12] as well as by 230 °C at *P*_{sb} = 200 W and a processing duration of 30 s [16].

The surface morphology of the films was studied via scanning electron microscopy (SEM) using a Supra 40 microscope (Carl Zeiss, Germany). The chemical analysis of the samples was performed by energy-dispersive X-ray (EDX) microanalysis with the aid of an INCA Energy attachment (Oxford Instruments). An accelerating voltage of 20 kV was used in the research. The studies were carried out on an area of 20 × 15 μm² with a normal incidence of the electron beam. This provided the collection of information from the entire thickness of the film. The reproducibility of the results on different parts of the film surface was high, and the deviations in the determined Cu/Se ratio did not exceed 2%. The X-ray diffraction (XRD) studies were performed using an ARL X'tra (Switzerland) diffractometer for Cu K_α radiation. The step-scan mode was used with a step size of 0.02° and counting time of 1.5 s per step.

3. Results and Discussion

The initial state of the investigated copper selenide films has a nontrivial structure. A typical initial film surface and the cross-section of the film shown in Figure 1. The films consist of nanocrystallites with dimensions of 50–120 nm connected in large clusters. There are large sinuous pores between the clusters. This structure of the copper selenide films is common and occurs in various growth methods [17–21]. In the cross-sectional image (Figure 1c), two layers are clearly distinguishable by the film thicknesses. The lower layer has a thickness of approximately 630–650 nm, larger crystallites, and larger pores, while the upper layer has a thickness of approximately 220 nm, smaller crystallites, and smaller pores. The XRD patterns of the initial state within the 2θ range of 5–90° are shown in Figure 2. The characteristic peaks correspond to the (111), (200), (220), (311), (400), (331), (422), and (511) lattice planes of cubic phase (Fm-3m) Cu_{1.75}Se to with high accuracy according to the values in ICDD card 01-075-2714. No other phases were observed in the studied layers. Notably, the highest intensity (Figure 2) is characteristic of the (111) plane, i.e., the growth of the crystallites occurs mainly in the [111] direction of the cubic structure, which is typical for Cu_{2-x}Se films [20–22]. The EDX data indicate that the ratio of Cu:Se atoms in the copper selenide films after growing and annealing is 1.75:1.00; hence, the chemical composition of the films deposited by this method can be identified as Cu_{1.75}Se.

A comparison of the chemical compositions obtained by the XRD and EDX methods is in good agreement with the results. Thus, the copper selenide films in the initial state have a chemical composition of $\text{Cu}_{1.75}\text{Se}$, and are characterized by a nanocrystalline structure with a complex architecture and large pore volume.

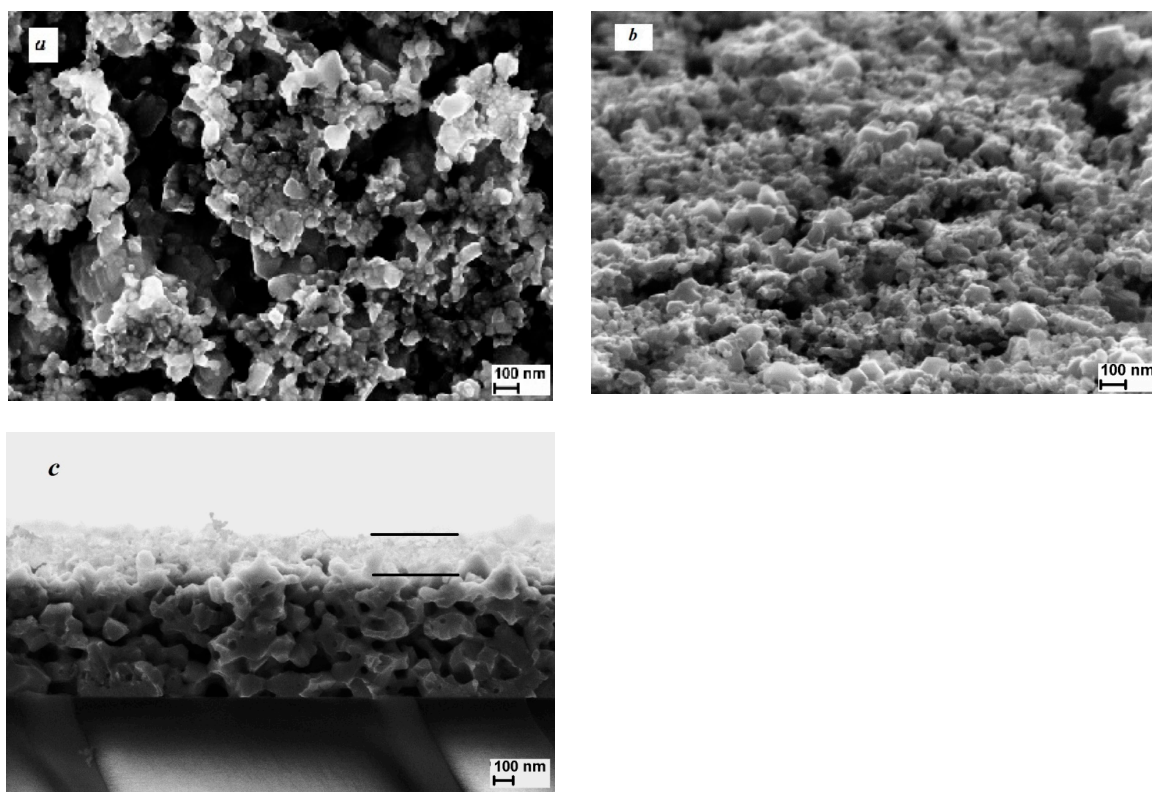


Figure 1. SEM images of the surface (a,b) and cross-section (c) of the film in a pristine state. The sample tilt during imaging was (a) 0° and (b) 70°.

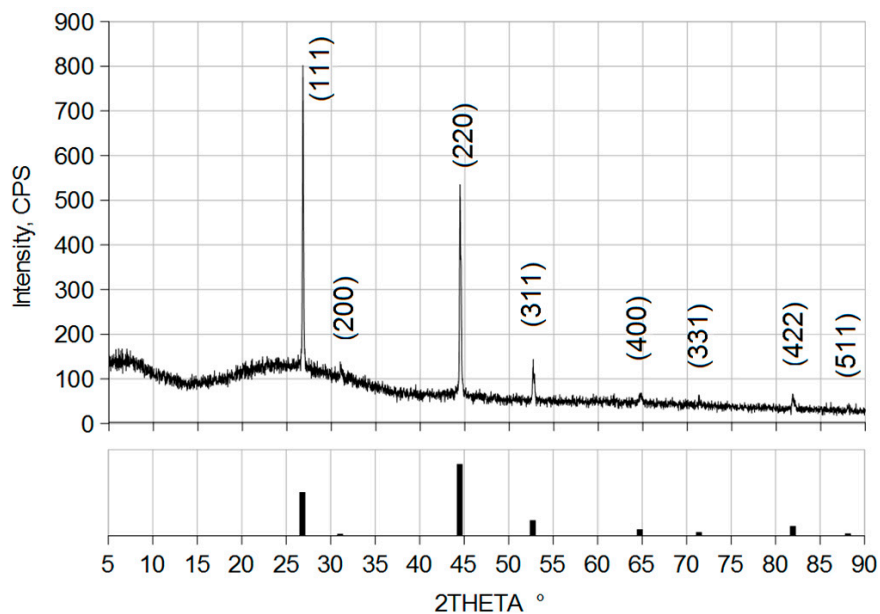


Figure 2. XRD pattern of the film in the initial state. The bottom of the plot shows the details of the ICDD card 01-075-2714 for $\text{Cu}_{1.75}\text{Se}$.

Ion sputtering in argon plasma led to significant changes in the surface morphology of the studied films. The dynamics of these changes during sputtering by 25 eV argon ions over a time interval of 30–90 s are shown in Figure 3. We consider an image taken normal to the surface, an image of a tilted surface and a cross-sectional image of the film/substrate. As shown in Figure 3b, when the process time was 30 s, vertical cone-shaped structure arrays were formed on the surface. The density of these cones is approximately $7 \times 10^9 \text{ cm}^{-2}$, and the angle of the cone at the top varies between 25–50°. Thus, a short duration of exposure to argon ions leads to the restructuring of previously formed copper selenide clusters and appearance of high (180–250 nm) cones. The height of these cones corresponds approximately to the thickness of the top layer in Figure 1c.

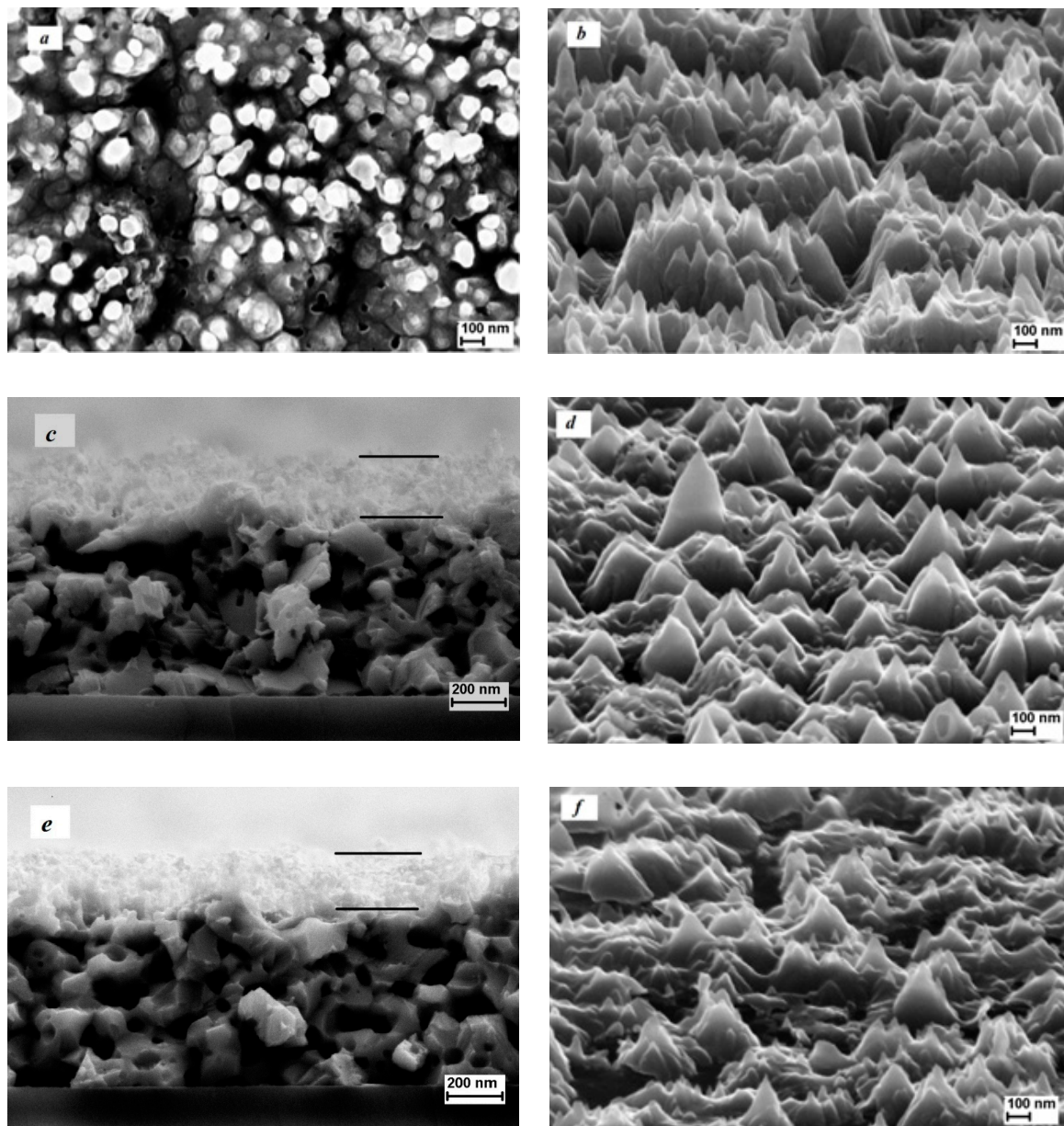


Figure 3. SEM images of the copper selenide film surface after plasma treatment at ion energy of 25 eV and durations of 30 s (a,b), 60 s (c,d), and 90 s (e,f). The sample tilts during imaging were 0° (a) and 70° (b,d,f). (c,e) Cross-sections of film, where the black lines are the borders of the lower and upper layers.

Several explanations for the appearance of micro- and nanocones have been proposed in experimental and theoretical ion sputtering studies [23,24]. However, these explanations

are all based on the compact materials. In our case, it is necessary to consider both the complex porous structure of the surface and re-deposition processes of the chemical elements that lead to the formation of local masks. The ions in a dense homogeneous ion stream perform different functions when they interact with a porous surface. Some of the ions result in the sputtering of clusters on the surface. The other ions, which fall into the pore areas, participate in the etching of the material in the film bulk, and remove the thin partitions in the porous structure. Sputtering processes are known to be accompanied by the re-deposition of sputtered chemical elements on the surface, self-organization of local masks, plasma-stimulated coalescence of nanoparticles, and densification of the porous material [25,26]. In [27], it was shown that, during the initial stage of ion sputtering of complex compounds containing copper and selenium, self-formation of copper-rich nanoparticles occurs. The nanoparticles later serve as local masks in the formation of cones. A similar situation occurs in our case. The rapid heating of the surface during plasma treatment and the influence of argon plasma ultraviolet radiation play an additional role in the ongoing processes. Consequently, arrays of vertical structures are formed. In a previous study, we described the formation of vertical nanostructures with the petal-shaped plate nanocrystallites on porous surfaces during the plasma sputtering of SnS films [28]. However, in the case of SnS, there is an important additional vapor–liquid–crystal mechanism during the vertical structures formation. Similar experimental results with the formation of vertical structures have been reported in porous boron and tungsten powders [29]. From the analysis of Figure 3, it can be seen that, when the exposure times were increased to 60 and 90 s (Figure 3c–f), the cone-shaped structures arrays on the surface were preserved; however, the height of the cones decreased, and the angle at the top of the cone increased. The latter is due to the prevalence of the process of sputtering the cones in this time interval. The analysis of the cross-section images shows that the ensemble of cones is still located in the upper layer of the film. If we consider the tops of the cones, the overall decrease in the film thickness is extremely small. This indicates that the sputtering processes in Cu_{1.75}Se films at the ion energy of 25 eV are weakly expressed, and that the local masks on the tops of cones are practically not etched.

We observe a different situation when the energy of the argon ions increased to 200 eV. A set of SEM images for the sputtering duration of 30–90 s is shown in Figure 4. The physical processes described above for the ion energy of 25 eV were repeated for ions with an energy of 200 eV and a sputtering duration of only 30 s. Within such a short duration, the sputtering still affected only the top layer of the film. At the processing time of 60 s, the top layer of the film was completely etched (Figure 4c), and at a processing time of 90 s, the lower layer of the film is etched (Figure 4e). The etching rate became uniform over the sample area, and was approximately 3 nm/s.

The changes in the surface morphology of Cu_{1.75}Se films during plasma treatment are accompanied by changes in the composition and crystal structure of the layers. EDX studies have shown that if the ratio of Cu/Se atoms was initially 1.75, then after sputtering by 25 eV ions for 60–90 s, the ratio became 1.87–1.88. Further, after plasma treatment by 200 eV ions for 60–90 s, the ratio increases to 1.98–2.01. Thus, the process of sputtering Cu_{1.75}Se nanocrystalline porous films by argon ions decreases the number of chalcogen atoms. From a physical perspective, this decrease is due to both the peculiarities of the copper selenide sputtering process and the effect of heating the sample during plasma treatment. Within the framework of linear cascade theory [30] the ratio of partial sputter yields Y_{Se}/Y_{Cu} is determined by the surface concentrations N_{Se}^S , N_{Cu}^S , surface binding energies U_{Se} , U_{Cu} , and masses M_{Se} and M_{Cu} :

$$\frac{Y_{Se}}{Y_{Cu}} \approx \frac{N_{Se}^S}{N_{Cu}^S} \left(\frac{M_{Cu}}{M_{Se}} \right)^{2m} \left(\frac{U_{Cu}}{U_{Se}} \right)^{1-2m} \quad (1)$$

where m can be assumed to be zero at low ion energies of 25 and 200 eV of our experiment [30]. Unfortunately, no information exists on the values of the surface binding energies of Cu and Se atoms in Cu_{1.75}Se in the literature for accurate calculations. Hence, we used the corresponding values for the single-component materials as a rough estimate.

Consequently, sublimation heat values of 102.2 kJ/mol for Se and 337 kJ/mol for Cu from [31] were used. Thus, at $Y_{Se}/Y_{Cu} \gtrsim 1.8$, preferential sputtering of selenium occurs for the $Cu_{1.75}Se$ films. During the ion sputtering of a binary compound, the selenium atoms quickly leave the working area because of their high volatility, and do not participate in the re-deposition process at the surface. In addition, the film temperature increases during ion sputtering. It is well known that the additional heating of the sample can also lead to the reduction of the chalcogen content in copper selenide films and contribute to the transformation from $Cu_{2-x}Se$ to Cu_2Se [32–34].

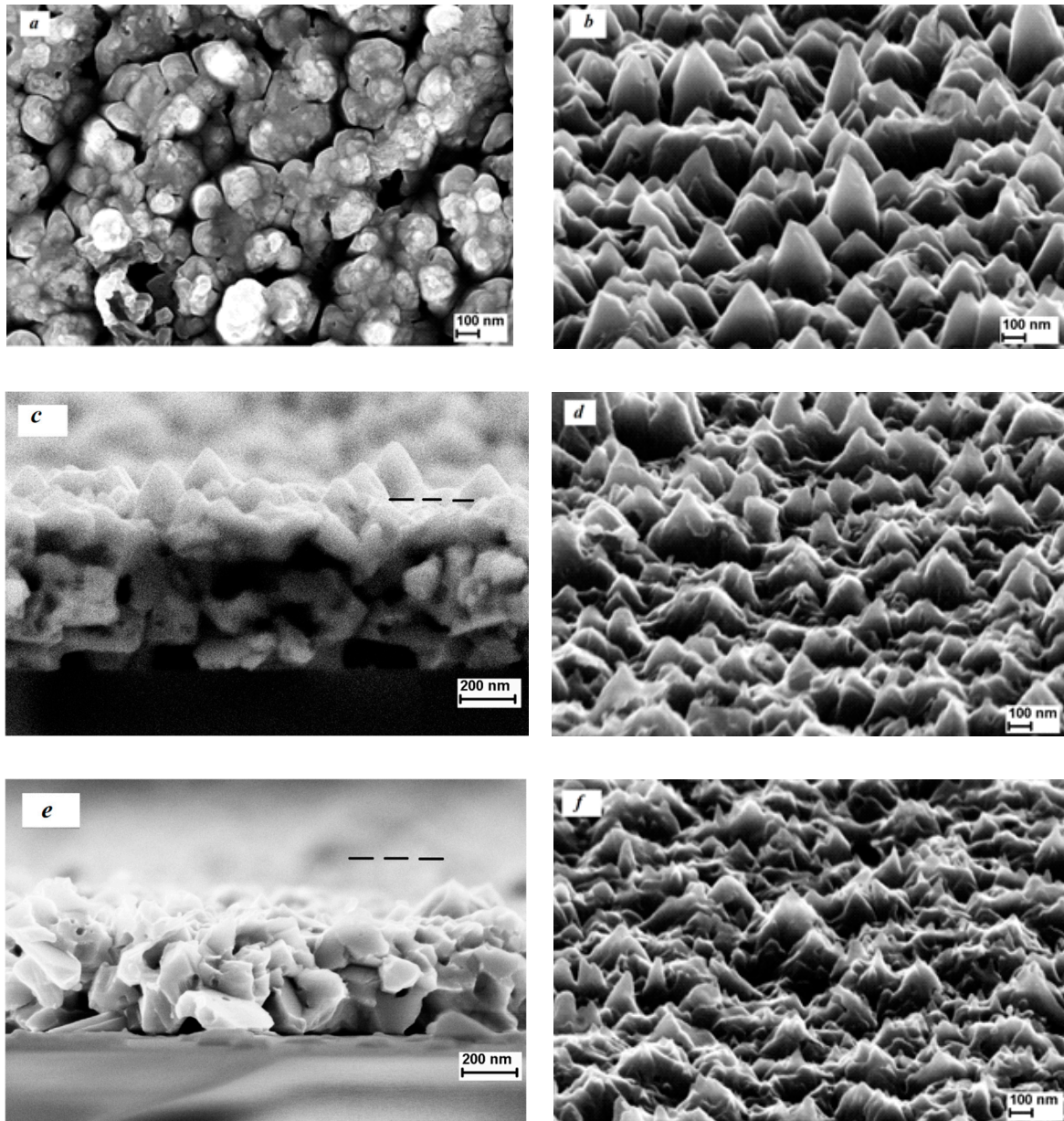


Figure 4. SEM images of the film surface after plasma sputtering at ion energy of 200 eV and processing times of 30 s (a,b), 60 s (c,d), and 90 s (e,f). The sample tilts during imaging were 0° (a) and 70° (b,d,f). (c,e) show cross-sections of the film. The dashed line in (c,e) shows the upper border of the lower layer in Figure 1c.

The X-ray diffractograms of the samples after plasma treatment at ion energies of 25 and 200 eV for durations of 60 and 90 s are presented in Figure 5. The results of the X-ray diffractometry indicate a change in the phase composition during ion sputtering.

In the initial state, the films were single-phase cubic crystal lattice $\text{Cu}_{1.75}\text{Se}$. After plasma treatment with 25 eV argon ions for 60 and 90 s, three phases appeared: cubic phase berzelianite $\text{Cu}_{1.78}\text{Se}$ (ICDD card 01-072-7490), monoclinic phase Cu_2Se (ICDD card 00-058-0228), and cubic phase berzelianite Cu_2Se (ICDD card 01-088-2043). After plasma treatment with 200 eV ions, two phases appeared in the diffractograms: monoclinic Cu_2Se phase (ICDD card 00-058-0228) and cubic Cu_2Se phase (ICDD card 01-088-2043). The coexistence of the cubic and monoclinic phases in Cu_{2-x}Se is expected and has been reported previously, for example, in bulk samples synthesized via conventional solid-state sintering technology in [35]. Thus, the results of X-ray diffractometry of Cu_{2-x}Se films, after plasma sputtering, are in good agreement with the EDX data, and confirm the transformation of $\text{Cu}_{1.75}\text{Se}$ to Cu_2Se during the Ar plasma treatment.

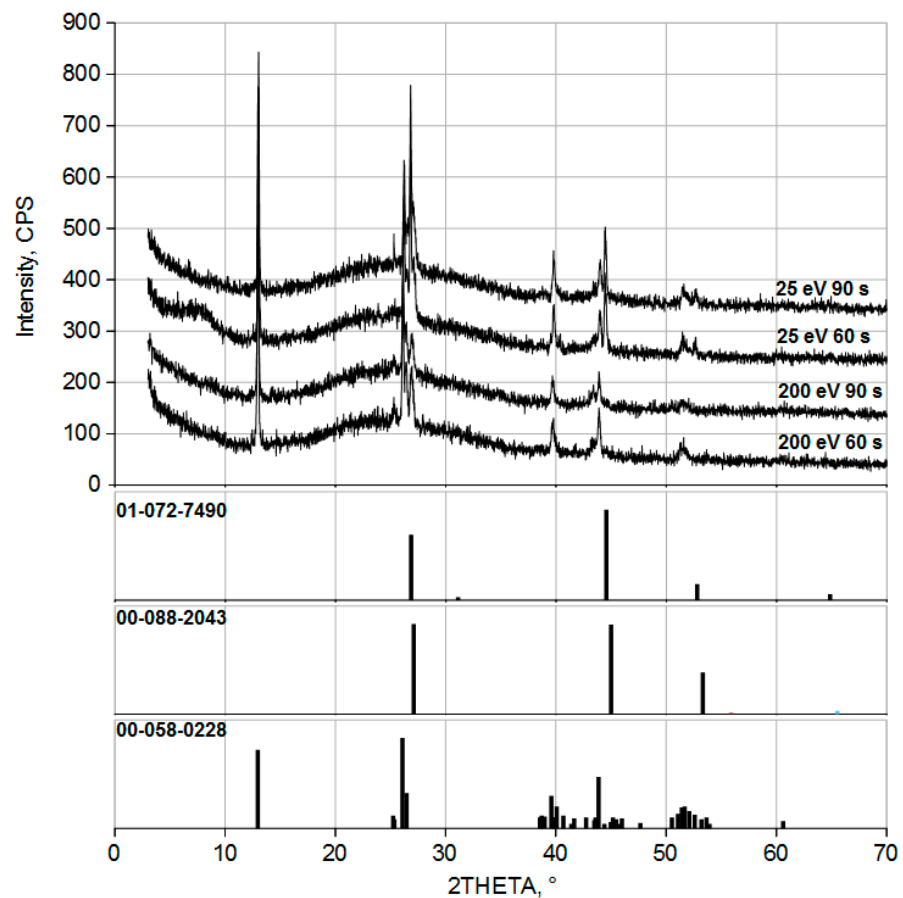


Figure 5. XRD patterns of the films after plasma treatment at ion energies of 25 and 200 eV. The bottom of the figure shows the ICDD card details for cubic phase $\text{Cu}_{1.78}\text{Se}$ (ICDD card 01-072-7490), cubic phase Cu_2Se (ICDD card 01-088-2043), and monoclinic phase Cu_2Se (ICDD card 00-058-0228).

4. Conclusions

The results show for the first time that ion-plasma sputtering is an effective method for modifying or removing surface layers in copper selenide films. The ion energy and process duration are significant. At an ion energy of 25 eV, local masks are formed on the surface, leading to the formation of ensembles of cones. When the ion energy is increased to 200 eV at longer process times, these local masks are peeled off and no high cones are formed. The etching process in argon plasma at ion energies of 25–200 eV is accompanied by a transformation of the phase composition of the films by the Cu_{2-x}Se -to- Cu_2Se mechanism. This transformation is due to the specific behavior of the metal and chalcogen atoms during ion-plasma treatment.

Author Contributions: Conceptualization, S.P.Z. and N.-H.K.; methodology, S.P.Z. and N.-H.K.; investigation, I.I.A., S.V.V., I.S.F., L.A.M., and N.-H.K.; data curation, I.I.A., S.V.V., and S.P.Z.; writing—original draft preparation, S.P.Z.; writing—review and editing, N.-H.K.; supervision, S.P.Z. and N.-H.K.; project administration, S.P.Z.; funding acquisition, S.P.Z. and N.-H.K. All authors have read and agreed to the published version of the manuscript.

Funding: This work was performed in the framework of the R&D initiative of Yaroslavl State University, project AAAA16-116070610023-3. The investigation was partially supported by Program no. 0066-2019-0002 of the Ministry of Science and Higher Education of Russian Federation for Valiev Institute of Physics and Technology of RAS. This work was supported by the Korea Institute of Energy Technology Evaluation and Planning (KETEP) and the Ministry of Trade, Industry and Energy (MOTIE) of the Republic of Korea (No. 20184010201650).

Informed Consent Statement: Not applicable.

Data Availability Statement: Data is contained within the article.

Acknowledgments: SEM and XRD investigations were carried out at the Facilities Sharing Center “Diagnostics of Micro- and Nanostructures” with the support of the Ministry of Science and Higher Education of Russian Federation.

Conflicts of Interest: The authors declare no conflict of interest. The founding sponsors had no role in the design of the study; in the collection, analyses, or interpretation of data; in the writing of the manuscript, and in the decision to publish the results.

References

1. Chen, X.; Yang, J.; Wu, T.; Li, L.; Luo, W.; Jiang, W.; Wang, L. Nanostructured binary copper chalcogenides: Synthesis strategies and common applications. *Nanoscale* **2018**, *10*, 15130–15163. [[CrossRef](#)] [[PubMed](#)]
2. Hussain, R.A.; Hussain, I. Copper selenide thin films from growth to applications. *Solid State Sci.* **2020**, *100*, 106101. [[CrossRef](#)]
3. Gan, X.Y.; Keller, E.L.; Warkentin, C.; Crawford, S.; Frontiera, R.; Millstone, J.E. Plasmon-Enhanced Chemical Conversion Using Copper Selenide Nanoparticles. *Nano Lett.* **2019**, *19*, 2384–2388. [[CrossRef](#)] [[PubMed](#)]
4. Singh, S.C.; Li, H.; Yao, C.; Zhan, Z.; Yu, W.; Yu, Z.; Guo, C. Structural and compositional control in copper selenide nanocrystals for light-induced self-repairable electrodes. *Nano Energy* **2018**, *51*, 774–785. [[CrossRef](#)]
5. Chen, Y.H.; Davoisne, C.; Tarascon, J.M.; Guery, C. Growth of single-crystal copper sulfide thin films via electrodeposition in ionic liquid media for lithium ion batteries. *J. Mater. Chem.* **2012**, *22*, 5295–5299. [[CrossRef](#)]
6. Chen, X.Q.; Li, Z.; Bai, Y.; Sun, Q.; Wang, L.Z.; Dou, S.X. Room-Temperature Synthesis of Cu_{2-x}E (E=S, Se) Nanotubes with Hierarchical Architecture as High-Performance Counter Electrodes of Quantum-Dot-Sensitized Solar Cells. *Chem. Eur. J.* **2015**, *21*, 1055–1063. [[CrossRef](#)]
7. Zhang, Y.; Hu, C.; Zheng, C.; Xi, Y.; Wan, B. Synthesis and Thermoelectric Property of Cu_{2-x}Se Nanowires. *J. Phys. Chem. C* **2010**, *114*, 14849–14853. [[CrossRef](#)]
8. Chen, D.H.; Chen, G.; Jin, R.C.; Xu, H.M. Self-decorated Cu_{2-x}Se nanosheets as anode materials for Li ion batteries and electrochemical hydrogen storage. *Cryst. Eng. Comm.* **2014**, *16*, 2810–2817. [[CrossRef](#)]
9. Choi, J.; Kang, N.; Yang, H.Y.; Kim, H.; Son, S.U. Colloidal Synthesis of Cubic-Phase Copper Selenide Nanodiscs and Their Optoelectronic Properties. *Chem. Mater.* **2010**, *22*, 3586–3588. [[CrossRef](#)]
10. Cao, H.L.; Qian, X.F.; Zai, J.T.; Yin, J.; Zhu, Z.K. Conversion of Cu_2O nanocrystals into hollow Cu_{2-x}Se nanocages with the preservation of morphologies. *Chem. Commun.* **2006**, *43*, 4548–4550. [[CrossRef](#)]
11. Cho, A.; Ahn, S.; Yun, J.H.; Gwak, J.; Ahn, S.K.; Shin, K.; Yoo, J.; Song, H.; Yoon, K. The growth of Cu_{2-x}Se thin films using nanoparticles. *Thin Solid Films* **2013**, *546*, 299–307. [[CrossRef](#)]
12. Zimin, S.P.; Amirov, I.I.; Naumov, V.V.; Guseva, K.E. The Formation of Hollow Lead Structures on the Surface of PbSe Films Treated in Argon Plasma. *Tech. Phys. Lett.* **2018**, *44*, 518–521. [[CrossRef](#)]
13. Zimin, S.P.; Gornachev, E.S.; Mokrov, D.A.; Amirov, I.I.; Naumov, V.V.; Gremenok, V.F.; Juskenas, R.; Skapas, M.; Kim, W.Y.; Bente, K.; et al. Surface nanostructuring of $\text{CuIn}_{1-x}\text{Ga}_x\text{Se}_2$ films using argon plasma treatment. *Semicond. Sci. Technol.* **2017**, *32*, 075014. [[CrossRef](#)]
14. Rasool, S.; Saritha, K.; Ramakrishna Reddy, K.T.; Tivanov, M.S.; Gremenok, V.F.; Zimin, S.P.; Pipkova, A.S.; Mazaletskiy, L.A.; Amirov, I.I. Annealing and plasma treatment effect on structural, morphological and topographical properties of evaporated $\beta\text{-In}_2\text{S}_3$ films. *Mater. Res. Express* **2020**, *7*, 016431. [[CrossRef](#)]
15. Kim, S.; Kim, N.-H. Impurity Phases and Optoelectronic Properties of CuSbSe_2 Thin Films Prepared by Cosputtering Process for Absorber Layer in Solar Cells. *Coatings* **2020**, *10*, 1209. [[CrossRef](#)]
16. Zimin, S.; Gornachev, E.; Amirov, I. Inductively Coupled Plasma Sputtering: Structure of IV-VI Semiconductors. In *Encyclopedia of Plasma Technology*, 1st ed.; Shohet, J.L., Ed.; CRC Press: New York, NY, USA, 2017; pp. 679–691. Available online: <https://www.routledgehandbooks.com/doi/10.1081/E-EPLT-120053966> (accessed on 1 November 2020).

17. Ghosh, A.; Kuls, C.; Banerjee, D.; Mondal, A. Galvanic synthesis of Cu_{2-x}Se thin films and their photocatalytic and thermoelectric properties. *Appl. Surf. Sci.* **2016**, *369*, 525–534. [CrossRef]
18. Zhou, R.; Huang, Y.; Zhou, J.; Niu, H.; Wan, L.; Li, Y.; Xu, J.; Xu, J. Copper selenide (Cu_3Se_2 and Cu_{2-x}Se) thin films: Electrochemical deposition and electrocatalytic application in quantum dot-sensitized solar cells. *Dalton Trans.* **2018**, *47*, 16587–16595. [CrossRef]
19. Ramesh, K.; Bharathi, B.; Thanikaikarasan, S.; Mahalingam, T.; Sebastian, P.J. Growth and Characterization of Electroplated Copper Selenide Thin Films. *J. New Mater. Electrochem. Syst.* **2013**, *16*, 127–132. [CrossRef]
20. Fedorova, E.A.; Maskaeva, L.N.; Markov, V.F.; Bamburov, V.G.; Voronin, V.I. Morphology and Thermal Stability of Thin $\text{Cu}_{1.8}\text{Se}$ Films Produced by Chemical Deposition. *Inorg. Mater.* **2019**, *55*, 106–115. [CrossRef]
21. Liu, K.; Jing, M.; Zhang, L.; Li, J.; Shi, L. Characterization of the phases and morphology in synthesizing Cu_{2-x}Se and CuSe films. *Integr. Ferroelectr.* **2018**, *189*, 71–77. [CrossRef]
22. Bhuse, V.M.; Hankare, P.P.; Garadkar, K.; Khomane, A. A simple, convenient, low temperature route to grow polycrystalline copper selenide thin films. *Mater. Chem. Phys.* **2003**, *80*, 82–88. [CrossRef]
23. Carter, G.; Navinsek, B.; Whitton, H.L. Heavy ion sputtering induced surface topography development. In *Sputtering by Particle Bombardment II*; Berish, R., Ed.; Topics in Applied Physics; Springer: Berlin/Heidelberg, Germany, 1983; Volume 52, pp. 231–269. [CrossRef]
24. Whitton, J.L. Experimental Studies of Morphology Development. In *Erosion and Growth of Solids Stimulated by Atom and Ion Beams*, 1st ed.; Kiriakidis, G., Carter, G., Whitton, J.L., Eds.; Nato Science Series E; Springer: Dordrecht, The Netherlands, 1986; Volume 112, pp. 151–173. [CrossRef]
25. Krashennikov, A.V.; Nordlund, K. Ion and electron irradiation-induced effects in nanostructured materials. *J. Appl. Phys.* **2010**, *107*, 071301. [CrossRef]
26. Meinander, K.; Nordlund, K. Irradiation-induced densification of cluster-assembled thin films. *Phys. Rev. B* **2009**, *79*, 045411. [CrossRef]
27. Liu, C.-H.; Chen, C.-H.; Chen, S.-Y.; Yen, Y.-T.; Kuo, W.-C.; Liao, Y.-K.; Juang, J.-Y.; Kuo, H.-C.; Lai, C.-H.; Chen, L.-J.; et al. Large Scale Single-Crystal $\text{Cu}(\text{In,Ga})\text{Se}_2$ Nanotip Arrays for High Efficiency Solar Cell. *Nano Lett.* **2011**, *11*, 4443–4448. [CrossRef] [PubMed]
28. Zimin, S.P.; Goralchev, E.S.; Mokrov, D.A.; Amirov, I.I.; Gremenok, V.F.; Ivanov, V.A. Specific Features of Vapor–Liquid–Solid Nanostructure Growth on the Surface of SnS Films during Plasma Treatment. *Semiconductors* **2017**, *51*, 1728–1731. [CrossRef]
29. Begrambekov, L.; Grunin, A.; Zakharov, A. Powder modification under influence of heat, electric field and particle irradiation. *Nucl. Instrum. Methods B* **2015**, *354*, 282–286. [CrossRef]
30. Sigmund, P. Elements of Sputtering Theory. In *Nanofabrication by Ion-Beam Sputtering*, 1st ed.; Som, T., Kanjilal, D., Eds.; Pan Stanford Publishing: Singapore, 2013; pp. 1–40. [CrossRef]
31. Lide, D.R. *CRC Handbook of Chemistry and Physics*, 76th ed.; CRC Press: New York, NY, USA, 1995; pp. 3–320.
32. Piacente, V.; Scardala, P. A study on the vaporization of copper(II) selenide. *J. Mater. Sci. Lett.* **1994**, *13*, 1343–1345. Available online: <http://pascal-francis.inist.fr/vibad/index.php?action=getRecordDetail&idt=4245620> (accessed on 1 November 2020). [CrossRef]
33. García, V.M.; Guerrero, L.; Nair, M.T.S.; Nair, P.K. Effect of thermal processing on optical and electrical properties of copper selenide thin films. *Superf. Vacío* **1999**, *9*, 213–218.
34. Liew, J.Y.C.; Talib, Z.A.; Zainal, Z.; Kamarudin, M.A.; Osman, N.H.; Lee, H.K. Structural and transport mechanism studies of copper selenide nanoparticles. *Semicond. Sci. Technol.* **2019**, *34*, 125017. [CrossRef]
35. Geng, Z.; Shi, D.; Shi, L.; Li, Y.; Snyder, G.J.; Lam, K. Conventional sintered Cu_{2-x}Se thermoelectric material. *J. Materiomics* **2019**, *5*, 626–633. [CrossRef]